Technical University of Denmark

DTU

McStas

CAMEA

Analytical calculations for CAMEA

Author:

M. Markó

ESS

PAUL SCHERRER INSTITUT

PSI

EPFL

ÉCOLE POLYTECHNIQUE
FÉDÉRALE DE LAUSANNE

Contents

1 Introduction

1.1 Goal of calculating the analytical model of the instrument

CAMEA is a totally new instrument concept, thus its performance is not explored. Furthermore it is a complex instrument using many different analyser arrays in a wide angular range. For studying the performance of the instrument we use three approaches: McStas simulations, analytical calculations, and prototyping. Due to the complexity of the instrument all of the previously mentioned methods can have faults misleading us during the instrument development. We use Monte Carlo and analytical modeling to calculate and optimize the instrument, while the measurements on the prototype validate the model calculations, give informations about the background and reveals the problems arising in the treatment of data obtained in real inelastic measurements. The main goal of the analytical calculation is to reveal the effects of the different instrument parameters on the resolution and on the intensity of the instrument. For this, I calculate and analyze the basic resolutions, then I calculate the resolution ellipsoid.

1.2 Basic method

The resolution is locally a convolution. Since the total convolution function of CAMEA has many different contributions, the final resolution function will be close to a Gaussian. I use Gaussian functions to describe each of the partial resolution functions. These Gaussian functions have the same variance (second moment) as the functions describing properly parts of the instrument. i.e. a cylindrical sample can be described as a box function with H width vertically, and a sphere with d diameter horizontally in the calculation I use the Gaussians with the variances of $H^2/12$ and $d^2/16$ respectively. Since during the convolution of two functions the variances are additive, this simplification causes just a small error. The difference between the calculated and the real resolution function has two main contributions: there are parts of the instrument I can not calculate analytically (i.e. the divergence of the incident beam at the sample position), and that the final resolution function is not exactly Gaussian.

I investigate the effects of the following parts of the instrument:

- Pulse duration, and the effect of the pulse shaping chopper
- Lengths: source-sample, sample-analyser and analyser-detector distances
- Divergence at the sample position (as a parameter of the instrument)
- Sample size (height and width)
- Size of the analyser elements
- Resolutions (radial and tangential) of the detector system

1.3 Parameters out of optimization

There are some parameters of the instrument we cannot choose, or optimize. The pulse duration of the ESS is 2.86ms, the frequency of the source is 14Hz. The pulse shaping chopper is minimum 6.5m avay from the moderator, and the first analyser array cannot be closer to the sample than 100 cm. Due to the flexibility of the instrument the pulse shaping chopper should be close to the source, and due to the cost of the pyrolitic graphite analysers, the analysers should be as close to the sample as it is possible, thus I use the above mentioned values as fix parameters.

The analyser arrays select final energies between 2.5 meV and 8 meV (5.7 Å and 3.2 Å), and we want to see also the higher orders up to 32 meV (1.6Å).

2 Primary resolution

The duration of the pulse is τ. The length of the primary instrument is L. The wavelength of the neutrons starting at t=0s and arriving to the sample at t is: $\lambda = (h/m_n)\tau/L = 3.956\tau/l$ where λ is the wavelength in Å,

t is in ms, L is in meter. Thus assuming constant τ (independent on the wavelength), the wavelength resolution of the front end is constant (the time resolution is constant). Thus the relative wavelength resolution is inversely proportional to the wavelength. Since there is just a second order difference between the relative wavelength and relative k resolution, the absolute k resolution is proportional to the square of k. The relative energy resolution is two times larger than the relative k resolution thus the absolute energy resolution is proportional to $E^{1.5} \sim 1/\lambda^3$.

2.1 Resolution of the pulse shaping chopper

The transmission of a chopper at a given time is the non-covered area of the guide opening divided by the total area of the guide. In general the transmission function of a chopper after a given guide can be described by a zeroth order spline (only the values of the polynoms are equal at the meeting points) containing maximum second order polynoms. From the time dependent transmission one can calculate the variance of the transmission distribution. I use a Gaussian function with similar variance can in the further calculations. There is a more simple way to calculate the time resolution: Neglecting the height of the guide, we can calculate an effective angle (ϕ_e) for the guide which is equal to the rotation angle of the chopper needed for full opening or closing: $\phi_e = 2 * \arctan(w/(2h))$ where d is the width of the guide, and R is the distance between the middle of the guide opening and the rotation axis of the chopper. The transmission of the chopper is a convolution of two box function with the width of ϕ_e and ϕ (the opening angle of the slit). Using the corresponding Gaussian approximation, the FWHM of the transmission function in time is:

$$FWHM_{ch} = \frac{1}{f}\sqrt{\frac{\phi^2 + {\phi_e}^2}{2\pi}\frac{8\ln 2}{12}} \tag{1}$$

Where f is the frequency of the chopper in Hz, and $\sqrt{\frac{8\ln 2}{12}}$ is the change factor between a box function with unit width and the FWHM of the Gaussian having the same variance as the box function. The time resolution of the instrument is a bit larger since the pulse duration (seen by the sample) is the projected transmission in the flight time - flight path diagram (TOF diagram) from the sample to the source: the correction factor is:$L_p/(L_p - l_{ch})$ where L_p is the primary instrument length, and l_{ch} is the source - chopper distance. In other words we see a virtual source at the position of the pulse shaping chopper at 6.5 m. The total transmitted intensity is proportional to the minimum of ϕ and ϕ_e and inversely proportional to the frequency of the chopper (in the case of pulsed source). This calculation describes well the resolution and the transmission of the choppers as long as the neutron intensity is constant in time and in wavelength. Later I show that near the end of the wavelength band the finite pulse duration causes a decreasing of the intensity and also the resolution width.

2.2 Pulse shaping chopper and instrument length

The pulse shaping chopper can be used to decrease τ thus to improve the resolution. In the TOF diagram looking back from the sample position to the source the pulse shaping chopper will make a "shadow" covering parts of the source. In other words we see an effective source. The position of the pulse shaping chopper is 6.5m. This means, that the effective source will move as we change the wavelength (time at the sample). At two different times (difference is Δt) at the sample position the middle of the effective source will move by $-6.5/(L-6.5)\Delta t$. This means that if L is smaller than 169m, the effective source will move more than the pulse duration, thus applying strict pulse shaping, there will be no incident neutrons at the ends of the wavelength band since the effective source is outside of the real pulse (in time). So (without wavelength-multiplication method), the minimum length of the front end (the 'natural length') is 169m [4, 5]. In reality the duration of the neutron pulse is larger than the duration of the proton pulse (due to the asymmetric response function of the moderator) causing a bit smaller natural length. The maximal primary instrument length at ESS is 165m, thus we choose this value for our instrument. In this case the wavelength band is roughly 1.7Å, the absolute wavelength resolution (without using PSC) is roughly 0.048 Å and the energy resolution at 4 Å (5 meV) is 0.12 meV.

In reality the real resolution is a bit more difficult: The time resolution is constant only if there is no pulse shaping chopper applied, or if we use very narrow (almost totally closed) pulse shaping chopper. In other case the time resolution will be better at the ends of the wavelength band where one end of the pulse will be defined

by the real pulse duration not by the chopper (i.e. the shadow of the chopper is out of the pulse). This has to be taken into account in the calculations. The effect of a moderate pulse shaping is seen on the figure 2. The given parameters with infinitely long pulse duration would give constant 1.343 ms time resolution.

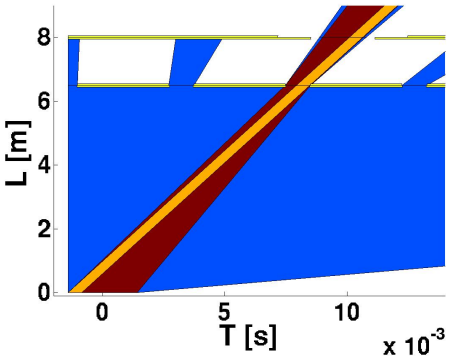

Figure 1: Effect of pulse shaping chopper at the end of the wavelength band: TOF diagram till the first two choppers of ESS CAMEA. The blue area shows the possible trajectories of the neutrons, the yellow lines show the choppers (double line is the fully closed, single line is the partially closed), the brown area shows the neutrons reaching the sample, and the orange area shows the neutrons arriving to the sample in one time at the end of the wavelength band. The time resolution in this case is much smaller than the opening of the pulse shaping chopper.

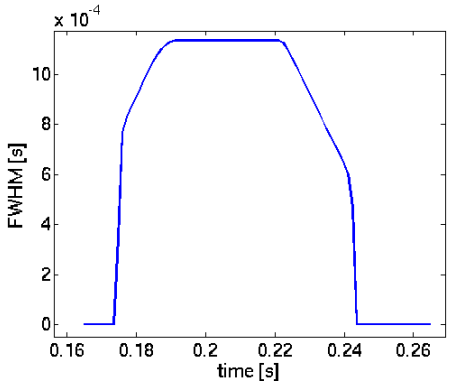

Figure 2: Effective FWHM of time-resolution for ESS-CAMEA: mean wavelength is 5Å PSC frequency is 210Hz, position is 6.5 m, opening angle is 150^o. The time resolution with infinitely long pulse would be 1.343 ms, the total chopper opening is 1.85 ms

By increasing the instrument length the resolution without PSC will be better and the energy band will be smaller. A two times longer instrument needs two separate measurement to cover the same (q or energy) range, but due to the longer length the PSC opening can be two times larger, so the intensity at the same resolution is larger (two times larger if the pulse duration is large enough). It has other advantages like smaller background and larger flexibility to use the PSC. However, the maximum total intensity (without using PSC) will be two times smaller due to the smaller wavelength band. As a consequence, the instrument length should be defined by the worst resolution (highest intensity) is still useful for measurements. In our case the worst resolution (0.17 meV at 165m without PSC) is useful, so the optimal length remains 170m. The same calculation is true for a two-times shorter instrument with frame multiplication. In this case the reachable highest intensity corresponds to a very bad resolution the flexibility of the instrument is worse, and the design is more difficult. **Finaly the maximal length (165 m) is also the optimal length for CAMEA.**

2.3 Calculation of the divergence of front end

There are two possibilities: Assuming constant intensity distribution one can calculate the minimum of the maximal divergence allowed by the guide opening or the last slit, and the maximum divergence transmitted by the guide system. The other possibility to use the results of McStas simulation. Note that the divergence is wavelength dependent. According to the experiences the first method frequently gives false data (if the collimation after the guide is not too strict), thus we checked the primary divergence by using MonteCarlo simulations.

3 Resolution of the secondary instrument

3.1 Energy resolution of the analysers

Assuming negligible variation of the lattice spacing, the derivation of the Bragg-law ($\lambda = 2d\sin(\theta)$) gives the relative resolution of one analyser crystal: $\frac{\Delta\lambda}{\lambda} = \Delta\Theta_a \cot\Theta_a$, where Θ_a is the scattering angle of the analyser and $\Delta\Theta_a$ is the angular resolution. Furthermore I calculate for focusing crystals in Rowland geometry. In Rowland geometry each crystal blade scatters the neutrons with the same energy, if the neutrons are coming from a point source (sample) and it focuses them to an other point (detector). Looking one crystal, the deviation from the scattering angle for a given path is half of the difference of the angular deviations before and after the analyser comparing to the nominal path (the path going through the center of sample, analyser and detector). Thus the change of the scattering angle is:

$$(\Theta_a - \Theta_{a0}) = \frac{1}{2}\left(\frac{x_s}{l_{sa}} + \frac{x_a(l_{sa} - l_{ad})}{l_{sa}l_{ad}} + \frac{x_d}{l_{ad}}\right) \tag{2}$$

where x_s, x_d are the positions perpendicular to the beam at the sample and detector respectively x_a is the position of on the analyser corrected with $\sin\theta_a$, l_{sa} and l_{ad} are the sample analyser and the analyser detector distances. For the same path (assuming elastic scattering) the angular deviation from the nominal q-direction is the half of the sum of divergences before and after the analyser:

$$\phi - \phi_0 = \frac{1}{2}\left(\frac{x_s}{l_{sa}} - \frac{x_a(l_{sa} + l_{ad})}{l_{sa}l_{ad}} - \frac{x_d}{l_{ad}}\right) \tag{3}$$

The analyser reflectivity, detector efficiency (as the function of the distance from the nominal beam) and mosaicity have the variances of s^2, a^2, d^2, m respectively. We can write the intensity of all of the paths corresponding to a given $(\Theta_a - \Theta_{a0})$ as a double integral (there are three parameters, but one is fixed by the equation 2. After calculating the integral we got also Gaussian intensity distribution in the function of $(\Theta - \Theta_0)$. The variance of the scattering angle distribution becomes:

$$\sigma^2_{\Theta_a} = \frac{m^2\left(s^2l_{ad}^2 + d^2l_{sa}^2 + a^2(l_{sa} + l_{ad})^2\right) + a^2d^2 + s^2d^2 + s^2a^2}{4m^2l_{sa}^2l_{ad}^2 + s^2l_{ad}^2 + d^2l_{sa}^2 + a^2(l_{sa} + l_{ad})^2} \tag{4}$$

If we take a large mosaicity value, then we get back the Rowland resolution:

$$\sigma^2_{\Theta_a} = \frac{s^2}{4l_{sa}^2} + \frac{a^2(l_{sa} + l_{ad})^2}{4l_{sa}^2l_{ad}^2} + \frac{d^2}{4l_{ad}^2} \tag{5}$$

Large mosaicity value means, that $\phi - \phi_0$ in the equation 3 is always smaller than the mosaicity (the distances are large enough, and the sample and detectors are small enough). In this case we are speaking about geometry limited resolution. At CAMEA the secondary resolution is geometry limited due to the large distances. The high resolution due to the large distances and good detector resolution does not affect the detected intensity: applying many detectors next to each others we cover the whole angular range of the neutrons scattered by the analyser, thus we analyse many different energies simultaneously [1]

Using the eq.5 the energy and radial $k_f$resolution due to the geometry is:

$$\sigma^2_{E_f} = E_f^2\cot^2(\Theta_a)\left(\frac{s^2}{l_{sa}^2} + \frac{a^2(l_{sa} - l_{ad})^2}{l_{sa}^2l_{ad}^2} + \frac{d^2}{l_{ad}^2}\right) \tag{6}$$

$$\sigma^2_{k_{fr}} = k_f^2\frac{\cot^2(\Theta_a)}{4}\left(\frac{s^2}{l_{sa}^2} + \frac{a^2(lsa - lad)^2}{l_{sa}^2l_{ad}^2} + \frac{d^2}{l_{ad}^2}\right) \tag{7}$$

So in the case of asymmetric Rowland geometry, the size of the crystals has a small effect on the energy resolution, while in symmetric case this is just a second order effect. As the equations show in optimal case $s/l_{sa} > 2d/l_{ad}$ meaning that the secondary resolution is defined mainly by the sample size thus the detected intensity is near proportional to the secondary resolution. As an example in symmetrical Rowland geometry the detector width (or resolution in the case of position sensitive detector) should be smaller than the sample. In the case of CAMEA at ESS this is possible but extremely expensive. The generally used tubes with the diameter of 1/2" will mostly define the resolution if the sample is smaller than 1 cm.

There is another second order effect on the resolution which is not taken into account. The analysers are straight. This means that the angle between the beam coming from the sample and the scattering plane depends on the position where the neutron reaches the crystal (the crystal is in tangential direction but it is not curved). That means that the scattering angle changes slightly but the effect of it is much smaller than the resolution of the analyser. Also the sample - analyser and the analyser - detector distances are changing, but the differences in the resolution are smaller than the accuracy of the analytical calculation.

It is important to note, that we use distance collimation meaning that the mosaicity of the analyser crystals does not effect the resolution. To detect every neutrons scatterecd by the analyser, we use more detectors next to each other looking the analyser from a slightly different angle. With this solution we can analyse many different energies using one analyser [1]. This also means, that the detected intensity depends only on the angular coverage of the analysers, and on the integrated reflectivity but not depends on the resolution of the secondary instrument.

3.2 Tangential $\mathbf{k}_f$resolution of the secondary instrument

This part of the resolution is produced by the width of the sample, the resolution of the detector (in tangential direction), the take-of angle of the detector, and the mosaicity.

The analyser banks contain flat analyser crystals. This means that after Bragg-reflection the horizontal divergence remains the same. The scattering angle (a4) can be calculated (in first order) using the total secondary flight path and the position of a count in the detector. Let us sign $a4_0$ the scattering angle in which direction the plane of the secondary flight path is vertical. In this case l_0 is the secondary flight path, and $x_0 = 0$ is the position on the detector. Then the scattering angle of the neutron arrived to the detector at x position is: $a4 = a4_0 + \arctan((x)/l_0)$. If the analyser width is not too large then we can simplify this function: $a4 = a4_0 + x/l_0$. In the case of resolution calculation the differences between the positions are small, so we use this last function.

The variance of the sample (S^2) and the resolution of the detector (D^2) has the same effect on the resolution, so resolution due to the geometry is:

$$(\sigma_{a4,g})^2 = \left(\frac{D}{L_s}\right)^2 + \left(\frac{S}{L_s}\right)^2 \tag{8}$$

Where $L_s = l_{sa} + l_{ad}$ is the total secondary flight path. The mosaicity has different effect: The mosaicity in the direction lying in the scattering plane of analyser has no effect on the tangential k_f-resolution. On the other direction (perpendicular to the scattering plane) it changes the direction of the scattered beam in the plane defined by the analyser and the detector. If an ideally collimated beam reaches the analyser then the reflected beam will be divergent: m mosaicity cause $\sigma_\phi = m2\sin\Theta_a$. This divergence causes a spot on the detector with the width of $\Delta x = \Delta\phi l_{ad}$ where l_{ad} is the analyser-detector distance. The tangential k_f resolution caused by the analyser is:

$$\sigma_{k_f,ta} = \frac{k\Delta x}{L_s} = q_a m \frac{l_{ad}}{L_s} \tag{9}$$

where q_a is the length of reciprocal lattice vector of the analyser. The total tangential $\mathbf{k}_f$resolution is:

$$\sigma_{kf}^2 = \left(\frac{q_a m l_{ad}}{L_s}\right)^2 + k_f^2\left(\frac{D}{L_s}\right)^2 + k_f^2\left(\frac{S}{L_s}\right)^2 \tag{10}$$

Equation 10 shows a uniqe property of the ESS CAMEA: the first part is indpendent of k_f, and implicitly the second and third parts are independent: k_f/L_s is inversely proportional to the secondary flight time what should be the same for each analyser due to the effective working of the order sorting choppers. As a result, the

tangential resolution of k_f is independent on the analysed energy, it is defined only by the ratio of the analyser-detector distance and the total secondary flight path. Moreover, if the primary divergence is proportional to the wavelength (since the critical angle of the mirror is proportional to it) then the final two dimensional q-resolution ellipsoid of the instrument caused by the angular resolution depends only on the scattering angle.

3.3 Time resolution of the secondary instrument

The time resolution consists two parts: the secondary flight path distribution, and the secondary energy resolution.

The secondary length distribution gives a part of the secondary TOF distribution. The sample size has two effects: the size in the direction of the primary beam causes a time distribution depending on the initial speed (energy), and the size in the scattered direction causes a time distribution depending on the analysed speed. The detection position distribution in the detector depends on the total cross section of the detector material, the detector width, shape and also on the speed of the analysed neutrons. These effects are smaller than 1 cm causing a maximum of some tens of μs time distribution calculating with the smallest incident and final speed. The last effect is the path distribution caused by the Rowland geometry. In figure 3 the radius of the Rowland circle divide the SAD angle to ϕ_1 and ϕ_2. Then the difference between the longest and shortest paths in first order is $d(\sin\phi_1 - \sin\phi_2)$ where d is the total width of the analyser. It is in extreme case 2d. Since we do not plan to use extremely asymmetric Rowland geometry, the flight path differences will be around some centimeters.

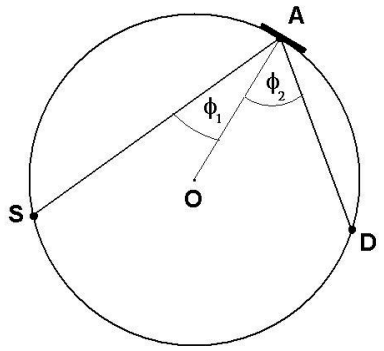

Figure 3: Rowland geometry: S: sample, A: analyser, D: detector, O: center of the rowland circle

The total time resolution (Δt_s) is calculated as:

$$\Delta t_s^2 = t_s^2 \left(\left(\frac{\Delta l_s}{l_s} \right)^2 + \left(\frac{\Delta E_f}{4E_f} \right)^2 \right) \tag{11}$$

where l_s and t_s are the secondary flight path, and flight time respectively.

4 Resolution ellipsoid

The calculation of the total resolution is based on the works of Cooper and Nathan [6], and Popovici [7]. The modifications I made are similar to the calculations of Ionita [9] and Violini[8]. The starting variables are the starting time, and the horizontal and vertical position at the end of guide, sample, analyser crystal and detector. An extra variable is the number of the crystals in one focusing analyser. I calculated the transformation from these variables to the q-ω space, and made the integration. I used the matrix formalism proposed by Popovici with a small change: Instead of using the transformations from step to step (from positions to divergences, from divergences the the six dimensional space of k_i and k_f, and to the q-ω space, I calculate the resolution matrix and then the covariance matrix (inverse of the resolution matrix) in the space spanned by the starting

parameters, and then I applied the coordinate transformation on the covariance matrix, getting the covariance matrix in the q-ω space. The final resolution matrix is the inverse of the covariance matrix.

The steps of calculation are:

- I describe the trajectory of the neutron by a 10 dimensional, vector ($\mathbf{x}$: starting time, position at the end of the guide, position of scattering on the sample, position of scattering on the analyser crystal, number of the analyser crystal, and the horizontal and vertical position of detection. (the number of analysers is also used as a continuous variable, it causes not significant error also in the original Popovici method).

- The first part of the resolution matrix is a diagonal matrix (R_0) containing the inverse of the variances of the starting parameters in the main axis.

- I calculate the divergence matrix D containing the divergence vectors (column vector): $\mathbf{d_i}$. $\mathbf{d_i}$ gives the angular deviation ($\Delta\phi_i = \mathbf{x}^T\mathbf{d_i}$) of the trajectories between two neutron optical elements. Before and after the analyser I calculate two kind of divergence: caused by one single analyser crystal, and the other is due to the focusing geometry. $\mathbf{x}^T D$ is a row vector containing all of the angular deviations. $\mathbf{d_0}$ is not a divergence it contains only the time (i.e. this vector is a unit vector, the first element is 1, and the others are zeros).

- The deviation of the scattering vectors on the analyser can be calculated as a linear combination of the divergences: M_i and M_o column vectors describe these linear transformations to get the angular deviation of the scattering vectors from the nominal one in the scattering plane and perpendicular to them. So, for a given trajectory these deviations are: $\mathbf{x}^T DM_i$ and $\mathbf{x}^T DM_o$

- The intensity distribution due to the divergencies and due to the mosaicities gives the second part of the resolution matrix: $R_d = \Sigma_j \mathbf{d}_j \mathbf{d}_j^T/\sigma_{dj}^2 + DM_i M_i^T D^T/\sigma_{mi}^2 + DM_o M_o^T D^T/\sigma_{mo}^2$ where σ_j^2 is the variance of the j-th divergence (where there is no extra restriction on the divergence (e.g. collimator), there σ_j is infinite, thus it does not count in the resolution matrix), σ_{mi}^2 andσ_{mo}^2 are the the mosaicities of the analyser in the scattering plane and perpendicular to it (variance, not FWHM).

- The total resolution matrix in the starting parameter space is: $R_p = R_0 + R_d$. The correlation matrix of the starting parameters is $C_p = R_p^{-1}$.

- The deviation of q-and E is also a linear combination of the divergences (and in our case also the starting time), I use the Q-matrix to describe this transformation, so for a trajectory given by $\mathbf{x}$ gives the $[\mathbf{q}; E]$ vector: $[\mathbf{q}; E] = \mathbf{x}^T DQ$. So, the transformation from the positions to the q-E space is described by the F=DQ.

- The resulting resolution matrix and correlation matrix in the q-E space are: $C = F^T C_p F$ and $R = C^{-1}$

The total q and E resolutions are the square root of the diagonal elements of the covariance matrix. The "Bragg resolutions" are the square root of the inverse of the diagonal elements of the resolution matrix. Bragg resolution shows the width of a curve we can get using a q or E scan over a Dirac-like scattering function (e.g. Bragg peak). The elastic resolution R_e is the 3X3 submatrix of R (not containing the 4th row and column), and the elastic covariance matrix C_e is the inverse of R_e.

This modified Popovici method claculated for TAS is mathematically equivalent with the original method, however it has some advantages:

- It is a bit more general, gives an easier procedure to calculate the resolutions for every kind of instrument

- The method gives the covariance matrix of the starting parameters. One can check whether a given optical element is too large or too small: if the given diagonal element of C_p is much smaller than the variance of the given parameter, then the corresponding optical element is larger than it should be. i.e. if the width of the guide end is 3cm, the variance of this parameter is 2, if the corresponding diagonal element of the covariance matrix is smaller than 4, then the guide is too large or the divergence transported by the guide is too small. In this case all of the neutrons exiting near the wall of the guide are useless, and they just increase the background. A smaller slit at the guide end does not effect the detected intensity nor the resolution, but decreases the background. Note that this effect can also be due to the intrinsic inaccuracy of the method (see below).

- Other kind of resolutions can be easily calculated like the time resolution of the secondary instrument for pulsed probe experiments. In this case the time resolution is also a linear combination of the starting parameters, the secondary flight time difference is $dt = \mathbf{x}^T\mathbf{t}$, thus the variance of the secondary flight time is: $\sigma_t^2 = \mathbf{t}^T C_p \mathbf{t}$.

Since this method differs from the original Popovici method only in the formalism, it has the same limitations. The most important ones are:

- The result is as correct as the input parameters are correct. The spatial and divergence distribution at the end of the guide (and the wavelength dependences of them) should be carefully investigated by McStas simulations.
- If there is one dominating part of the resolution (e.g. long pulse length), then the shape of the resolution function will be defined by the given partial resolution function, and it can be far from the Gaussian function.
- At some instruments (like backscattering spectrometer) the precise knowledge of the resolution function is needed in four order of dynamic range. In this case this method is good to predict the resolution during the instrument design, but the result cannot use as a convolution function at the actual data treatment.
- In some cases the Gaussian assumption gives better resolution than in the reality. e.g. at TAS if the guide end is close to the monochromator having the same size as the guide (and the divergence is small), the calculation shows a reduced useful area of the monochromator (like the monochromator of RITA II at PSI). In this case the artificially increased monochromator size in the calculation can result more realistic result. The small covariance matrix element (much smaller than the variance of the corresponding input parameter) can be due to the calculation method, or it can be due to real physical (or geometrical) cause. If the slight increasing of the input parameter does not effect the covariance matrix, then the given resolution is realistic. In other case the slight increasing of the input parameter causes half times large relative increasing of the corresponding diagonal element of the covariance matrix.

The projections of calculated and measured resolution ellipsoids for the prototype of CAMEA (built by DTU and installed in Mars instrument at PSI) can be found in [2] as an example three projection of the ellipsoid is shown in Figure 4. The basic resolutions are shown in the instrument proposal.

The projections of calculated resolution ellipsoids for the prototype of CAMEA (built by DTU and installed in Mars instrument at PSI) are seen in figure 4.

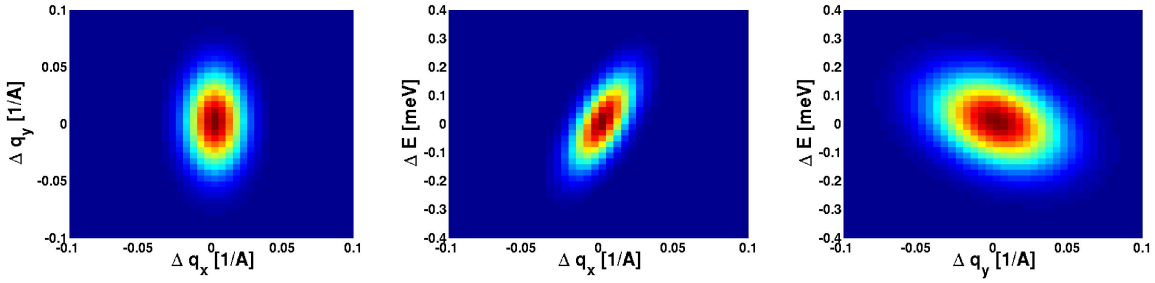

Figure 4: Projections of the resolution ellipsoid of one analyser-detector bank of the Prototype of CAMEA (elastic scattering, $E_i = 7$ meV $a_4 = 60^o$

5 Conclusions

The calculation method for the total resolution of CAMEA is presented. The calculations are validated by measurement on the prototype of CAMEA [2], and are in good agreement with McStas simulations [3]. We wrote a CAMEA object (in Matlab) containing all of the resolution calculations to help the final optimization of CAMEA. The secondary resolution can be calculated analytically, the primary divergence needs McStas

simulation, and the primary energy resolution needs numerical calculations due to the changing τ_{eff}. Altogether, with a given primary divergence the calculations are fast, and precise enough for the total optimization.

References

[1] J.O. Birk et al, in preparation for Nucl. Instr. Meth. A (2013)

[2] M. Marko, J. O. Birk Building and testing Prototype for CAMEA

[3] H. Ronnow et al. ESS Instrument Construction Proposal CAMEA

[4] K. Lefmann et al. Rev. Sci. Instr. 84, 055106 (2013)

[5] H. Schober et al., Nucl. Instr. Meth. A 589, 34 (2008)

[6] M.J. Cooper and R. Nathans, Acta Cryst. A29, 160-169.

[7] M. Popovici, Acta Cryst. A31, 507 (1975)

[8] N. Violini et al., Nucl. Instr. Meth. A. 736, 3139 (2014)

[9] I. Ionita Nucl. Instr. Meth. A. 513, 511523 (2013)